Chemistry and Physics of Lipids 226 (2020) 104849

Contents lists available at ScienceDirect

Chemistry and Physics of Lipids

journal homepage: www.elsevier.com/locate/chemphyslip

Differential sensitivity of pHLIP to ester and ether lipids

Bhagyashree D. Rao[a,b,c], Hirak Chakraborty[a,d], Arunima Chaudhuri[a,1], Amitabha Chattopadhyay[a,c,*]

[a] CSIR-Centre for Cellular and Molecular Biology, Uppal Road, Hyderabad, 500 007, India
[b] CSIR-Indian Institute of Chemical Technology, Uppal Road, Hyderabad, 500 007, India
[c] Academy of Scientific and Innovative Research, Ghaziabad, 201 002, India
[d] School of Chemistry, Sambalpur University, Jyoti Vihar, Burla, Odisha, 768 019, India

ARTICLE INFO

Keywords:
pHLIP
Ester lipids
Ether lipids
Membrane interaction
REES
Cancer biomarker

ABSTRACT

pH (low) insertion peptide (pHLIP) is a polypeptide from the third transmembrane helix of bacteriorhodopsin. The pH-dependent membrane insertion of pHLIP has been conveniently exploited for translocation of cargo molecules and as a novel imaging agent in cancer biology due to low extracellular pH in cancer tissues. Although the application of pHLIP for imaging tumor and targeted drug delivery is well studied, literature on pHLIP-membrane interaction is relatively less studied. Keeping this in mind, we explored the differential interaction of pHLIP with ester and ether lipid membranes utilizing fluorescence and CD spectroscopy. We report, for the first time, higher binding affinity of pHLIP toward ether lipid relative to ester lipid membranes. There results gain relevance since *Halobacterium halobium* (source of bacteriorhodopsin) is enriched with ether lipids. In addition, we monitored the difference in microenvironment around pHLIP tryptophans utilizing red edge excitation shift and observed increased motional restriction of water molecules in the interfacial region in ether lipid membranes. These changes were accompanied with increase in helicity of pHLIP in ether lipid relative to ester lipid membranes. Our results assume further relevance since ether lipids are upregulated in cancer cells and have emerged as potential biomarkers of various diseases including cancer.

1. Introduction

Biological membranes are complex two-dimensional, micro-heterogeneous fluids that contain a variety of lipids and proteins (Pal and Chattopadhyay, 2017). The majority of membrane functions are carried out by membrane proteins which also act as major drug targets (Drews, 2000; Dailey et al., 2009). A considerable portion of membrane proteins and peptides remains in close contact with membrane lipids, thereby allowing their function to be modulated by surrounding lipids, either *via* specific lipid-protein (or lipid-peptide) interaction or by modulation of membrane physical properties, or a combination of both mechanisms (Lee, 2004; Sanderson, 2005; Jafurulla et al., 2019). It is therefore essential to understand and appreciate the subtle interplay between membrane lipids and proteins (or peptides) to obtain a comprehensive understanding of membrane function. Fluorescence-based approaches have gained considerable popularity in monitoring lipid-peptide interaction due to their sensitivity, suitable time resolution and multiplicity of measurable parameters (Chattopadhyay and Raghuraman, 2004). In addition, the presence of naturally fluorescent tryptophans has helped in sensitive studies of lipid-peptide interaction using fluorescence-based spectroscopic approaches.

pH (low) insertion peptide (pHLIP) is a 36-residue polypeptide with the sequence GGEQNPIYWARYADWLFTTPLLLLDLALLVDADEGT (Fig. 1a), derived from the third transmembrane helix (helix-C) of bacteriorhodopsin (Hunt et al., 1997; Reshetnyak et al., 2007). The majority of amino acid residues in the peptide are hydrophobic in nature, except few charged residues that impart an overall charge of -5 at physiological pH (Rao et al., 2018). The amino acid sequence of pHLIP is responsible for its amphipathic nature, which is a common feature observed in membrane-interacting peptides. The presence of

Abbreviations: 2-AS, 2-9-anthroyloxystearic acid; 12-AS, 12-9-anthroyloxystearic acid; 5-PC, 1-palmitoyl-2-5-doxylstearoyl-*sn*-glycero-3-phosphocholine; 12-PC, 1-palmitoyl-2-12-doxylstearoyl-*sn*-glycero-3-phosphocholine; CD, circular dichroism; DMPC, 1,2-dimyristoyl-*sn*-glycero-3-phosphocholine; DODPC, 1,2-di-O-(9*Z*-octadecenyl-*sn*-glycero-3-phosphocholine; DOPC, 1,2-dioleoyl-*sn*-glycero-3-phosphocholine; LUV, large unilamellar vesicle; pHLIP, pH low insertion peptide; REES, red edge excitation shift; Tempo-PC, 1,2-dioleoyl-*sn*-glycero-3-phosphotempocholine

* Corresponding author at: CSIR-Centre for Cellular and Molecular Biology, Uppal Road, Hyderabad, 500 007, India.
E-mail address: amit@ccmb.res.in (A. Chattopadhyay).
[1] Present address: Department of Cell Biology, Yale University School of Medicine, New Haven, CT 06520, USA

https://doi.org/10.1016/j.chemphyslip.2019.104849
Received 24 October 2019; Received in revised form 5 December 2019; Accepted 5 December 2019
Available online 10 December 2019
0009-3084/

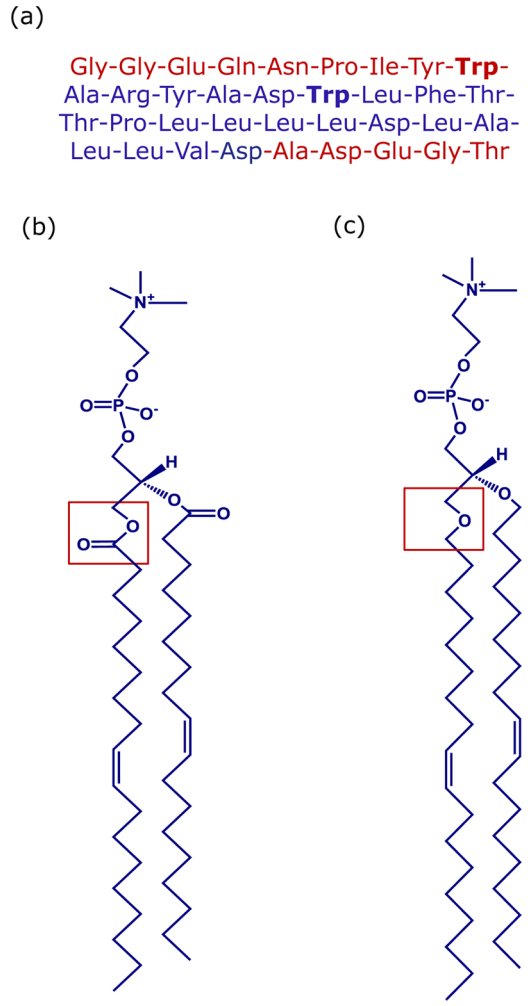

Fig. 1. Peptide sequence and structure of phospholipids used. (a) The amino acid sequence of pHLIP. The putative transmembrane region is shown in blue and the tryptophan residues are highlighted. Panels (b) and (c) show chemical structures of the phospholipids used (DOPC and DODPC, respectively). The ester and ether linkages in the phospholipids are highlighted.

two tryptophan residues makes pHLIP intrinsically fluorescent which facilitates the monitoring of peptide conformation, dynamics and membrane interaction utilizing fluorescence-based approaches.

A major attribute of pHLIP is its ability to exist in various conformations, which are dependent on peptide concentration, pH, and the presence of membranes (Reshetnyak et al., 2007). In aqueous solution (pH 8), pHLIP is unstructured and adopts a random coil conformation (denoted as state I), and upon interaction with lipids, is superficially adsorbed to membranes (state II). Lowering the pH to ~4 results in adoption of α-helical conformation, leading to spontaneous insertion of the peptide into membranes (state III) with the N-terminus on the extracellular side and the C-terminus on the intracellular side. It was previously shown that pHLIP insertion is triggered by protonation of four aspartate residues at acidic pH, which leads to an increase in peptide hydrophobicity and induces its insertion into membranes (Hunt et al., 1997; Reshetnyak et al., 2007). The mutation of the two aspartate residues (in the transmembrane region) was shown to result in loss of pH-dependent membrane insertion (Andreev et al., 2007). Recent studies utilizing a combination of spectroscopic approaches that include circular dichroism (CD), fluorescence and solid-state nuclear magnetic resonance (NMR) support a multistage model of pHLIP insertion into membranes (Scott et al., 2017; Otieno et al., 2018). The sequential protonation of four aspartate residues at distinct pH values triggers the formation of different intermediate states between the membrane-adsorbed and inserted forms of pHLIP. Alteration of positions of aspartate residues in pHLIP led to changes in the pKa of membrane insertion, suggesting the role of these residues in the membrane-translocated conformation of pHLIP (Fendos et al., 2013).

The pH-dependent membrane insertion of pHLIP has been successfully utilized for the translocation of cargo molecules (such as phalloidin and fluorescent cyclic hexapeptides) across the membrane bilayer at low pH (Reshetnyak et al., 2006; Thévenin et al., 2009; An et al., 2010). Apart from intracellular delivery of cargo molecules, pHLIP has been successfully used as a novel imaging agent in cancer biology since low (acidic) extracellular pH is a feature associated with tumor tissues (Reshetnyak et al., 2011; Adochite et al., 2014; Deacon et al., 2015; Burns et al., 2015; Wyatt et al., 2017). The use of pHLIP in tumor imaging and targeted intracellular delivery is convenient and effective, since the trigger for insertion can be easily modulated, with the inserted form not affecting membrane integrity (Zoonens et al., 2008), or cellular toxicity (Andreev et al., 2007).

Knowledge of the aggregation behavior of pHLIP is essential before monitoring and quantifying its interaction with membranes. Previous work has shown that pHLIP exists in the monomeric form up to a concentration of ~7 μM beyond which it undergoes aggregation (Reshetnyak et al., 2007; Rao et al., 2018). Several studies on the binding of pHLIP to membranes have provided useful insights into the intermediate states (Otieno et al., 2018), free energy of transition between the different states (Reshetnyak et al., 2008), topology (Reshetnyak et al., 2007) and kinetics of membrane insertion and exit (Tang and Gai, 2008; Andreev et al., 2010; Karabadzhak et al., 2012). The pH-dependence of membrane insertion and binding exhibited by pHLIP makes it a suitable model peptide for exploring lipid-peptide interaction.

In this work, we utilized the intrinsic fluorescence of tryptophan residues (located at positions 9 and 15) of pHLIP (Fig. 1a), to monitor the differential interaction of pHLIP with representative ester- and ether-linked phospholipid membranes (Fig. 1(b,c)). This assumes relevance since native membranes of bacteriorhodopsin (from where pHLIP is derived) are enriched in ether lipids (Kates et al., 1965; Marshall and Brown, 1968; Henderson, 1977; Renner et al., 2005). Earlier work utilizing fluorescence spectroscopy, infrared spectroscopy, monolayer studies and differential scanning calorimetry have reported differences in membrane organization of ester- and ether-linked phospholipids (Smaby et al., 1983; Mattjus et al., 1996; Lewis et al., 1996; Mukherjee and Chattopadhyay, 2005). Since the physicochemical properties of the interfacial region, which depend on the type of linkage (*i.e.* ester *vs* ether; see Fig. 1(b,c)) of the acyl chains to the glycerol backbone, could modulate peptide conformation and binding, we monitored the interaction of pHLIP to ester- and ether-linked lipid membranes. Our results show that membrane-inserted pHLIP exhibits higher affinity to ether-linked membranes relative to ester-linked membranes. Importantly, pHLIP tryptophans exhibited differential red edge excitation shift (REES) in ester and ether lipid membranes in the membrane-inserted form, clearly highlighting the difference in microenvironment experienced by these tryptophans. These observations are supported by increased helicity of pHLIP bound to ether lipid compared to ester lipid membranes, as monitored by CD measurements. Taken together, our results constitute the first report where differential interaction of pHLIP bound to membranes of ether- and ester-linked lipids is reported. More importantly, these results assume greater relevance since ether lipids are upregulated in cancer cells (Snyder and Wood, 1969; Howard et al., 1972; Albert and Anderson, 1977; Roos and Choppin, 1984; Benjamin et al., 2013; Jaffrès et al., 2016) and therefore have emerged as potential biomarkers in cancer pathophysiology.

2. Materials and methods

2.1. Materials

1,2-Dioleoyl-*sn*-glycero-3-phosphocholine (DOPC), 1,2-di-O-(9*Z*-octadecenyl)-*sn*-glycero-3-phosphocholine (DODPC), 1,2-dioleoyl-*sn*-glycero-3-phosphotempocholine (Tempo-PC), 1-palmitoyl-2-(5-doxyl) stearoyl-*sn*-glycero-3-phosphocholine (5-PC), and 1-palmitoyl-2-(12-doxyl)stearoyl-*sn*-glycero-3-phosphocholine (12-PC) were obtained from Avanti Polar Lipids (Alabaster, AL). 2-(9-Anthroyloxy)stearic acid (2-AS) and 12-(9-anthroyloxy)stearic acid (12-AS) were purchased from Molecular Probes/Invitrogen (Eugene, OR). 1,2-Dimyristoyl-*sn*-glycero-3-phosphocholine (DMPC), urea (BioUltra grade) and dialysis kit (PURD10005) with 1 kDa cut-off were purchased from Sigma Chemical Co. (St. Louis, MO). All other chemicals used were of the highest purity available. Water was purified through a Millipore (Bedford, MA) Milli-Q system and used throughout. Details of phospholipid assay, thin layer chromatography and peptide synthesis are provided in Supplementary Material (see section S1).

2.2. Preparation of peptide solutions

pHLIP was dissolved in buffer containing 6 M urea by intermittent vortexing (~10 min) at room temperature (~23 °C) as the peptide is hydrophobic in nature and susceptible to aggregation (Reshetnyak et al., 2007; Rao et al., 2018). Urea was removed from the peptide solution by dialysis as described previously (Rao et al., 2018). Concentration of pHLIP was estimated from its molar extinction coefficient (ε) of 13,940 M^{-1} cm^{-1} at 280 nm (Reshetnyak et al., 2007). Working stocks (2 or 5 μM) of the peptide were freshly prepared at pH 4 (10 mM citrate/phosphate buffer) or pH 8 (10 mM phosphate buffer) from secondary stock solutions (~10 μM).

2.3. Sample preparation

All experiments (except depth measurements) were performed with large unilamellar vesicles (LUVs) of 100 nm diameter of DOPC or DODPC, as described previously (Chaudhuri and Chattopadhyay, 2014). The concentration of pHLIP was kept constant at 2 μM, while the lipid concentration was varied from 25 to 600 μM for binding experiments utilizing tryptophan fluorescence. For CD measurements, peptide concentration was 5 μM, whereas the lipid concentration was 750 μM, to maintain the lipid/peptide ratio of 150 (mol/mol). To incorporate pHLIP into membranes, an aliquot of the peptide from a freshly prepared stock (either at pH 4 or 8) was added to the pre-formed vesicles and mixed well. See Supplementary Material (section S2) for more details.

2.4. Binding studies utilizing tryptophan fluorescence

Steady state fluorescence measurements were performed using a Fluorolog-3 Model FL-3-22 spectrofluorometer (Horiba Jobin Yvon, Edison, NJ) in the corrected spectrum mode, as described previously (Chakraborty and Chattopadhyay, 2017). pHLIP was incorporated into DOPC or DODPC membranes by adding an aliquot from a working stock solution (either pH 4 or pH 8) to the pre-formed vesicles. Data obtained were fitted to a simple hyperbolic function utilizing Sigma Plot (Systat Software Inc., San Jose, CA), according to the following equation:

$$F/F_o = B_{max}\,[Lipid]/(K_d + [Lipid]) \quad (1)$$

where F_o is the fluorescence intensity in buffer, F is the fluorescence intensity in the presence of lipid vesicles (at various concentrations), B_{max} is the maximum binding and K_d is the apparent dissociation constant for binding of pHLIP to membranes.

2.5. REES measurements

REES measurements utilizing tryptophan fluorescence of the membrane-inserted form of pHLIP (at pH 4) were performed in a Fluorolog-3 Model FL-3-22 spectrofluorometer (Horiba Jobin Yvon, Edison, NJ) as described previously (Chakraborty and Chattopadhyay, 2017).

2.6. Depth measurements using the parallax method

Membrane penetration depths of pHLIP tryptophans were estimated by the parallax method (Chattopadhyay and London, 1987). The actual spin (nitroxide) contents of the spin-labeled phospholipids (Tempo-, 5- and 12-PC) were assayed using fluorescence quenching of anthroyloxy-labeled fatty acids (2- and 12-AS) as described previously (Abrams and London, 1993). Liposomes were made by the ethanol injection method (Kremer et al., 1977) and depth measurements were performed as described previously (Chaudhuri and Chattopadhyay, 2014), with some modifications. pHLIP was incorporated into membranes by adding an aliquot from a freshly prepared working stock solution (pH 4) to the pre-formed vesicles such that the lipid/peptide ratio was 200 (mol/mol). See Supplementary Material (section S3) for more details.

2.7. Circular dichroism (CD) measurements

CD measurements were performed at room temperature (~23 °C) on a Chirascan Plus Spectropolarimeter (Applied Photophysics, Surrey, UK) calibrated with (+)-10-camphorsulfonic acid (Chen and Yang, 1977), as described previously (Rao et al., 2018). Spectra were recorded in 0.2 nm wavelength increments with a band width of 2 nm and an integration time of 2 s. The CD spectra of pHLIP in membranes were deconvoluted using the web-based CD analysis tool, DichroWeb (Whitmore and Wallace, 2004, 2008), applying the CDSSTR method (Sreerama and Woody, 2000) and using SP175 (Lees et al., 2006) as the reference data set for analysis. See Supplementary Material (section S4) for more details.

3. Results

3.1. Fluorescence emission characteristics of pHLIP tryptophans and binding in ester and ether lipid membranes

Tryptophan fluorescence is sensitive to its microenvironment (Kirby and Steiner, 1970; Eftink, 1991; Chattopadhyay et al., 2005), thereby making it an appropriate reporter of pHLIP binding to membranes composed of ether- and ester-linked lipids. The fluorescence emission spectra of tryptophans in membrane-inserted pHLIP (state III) in DOPC (ester-linked) and DODPC (ether-linked) lipid membranes at pH 4 are shown in Fig. 2. The fluorescence emission spectrum of pHLIP in pH 4 buffer is also shown. The figure shows that the fluorescence emission maximum (We have used the term maximum of fluorescence emission in a broad sense here. In every case, we have monitored the wavelength corresponding to maximum fluorescence intensity, as well as the center of mass of the fluorescence emission, in the symmetric part of the spectrum. In most cases, both these methods yielded the same wavelength.) of pHLIP in buffer was 333 nm. The emission maximum of membrane-inserted pHLIP in both DOPC and DODPC membranes was found to be 330 nm, displaying a 3 nm blue shift due to membrane insertion. The inset shows the shift in fluorescence emission maximum for pHLIP upon binding to DOPC and DODPC membranes.

The change in normalized fluorescence intensity of membrane-inserted pHLIP in DOPC and DODPC membranes with increasing lipid/peptide ratio (mol/mol) at pH 4 is shown in Fig. 3. The figure shows that fluorescence intensity exhibits progressive increase upon increasing lipid/peptide ratio (i.e., with increasing lipid concentration, since peptide concentration is kept constant), thereby indicating increase in population of bound peptide with increasing lipid

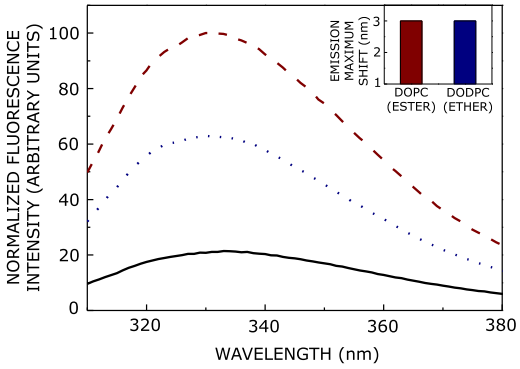

Fig. 2. Fluorescence emission characteristics of membrane-inserted pHLIP in ester and ether lipid membranes at pH 4. Representative fluorescence emission spectra of pHLIP in DOPC (·····) and DODPC (- - -) membranes. The emission spectra of pHLIP in buffer (—) at pH 4 is also shown. The inset shows the shift in fluorescence emission maximum for pHLIP upon binding to DOPC and DODPC membranes. The concentration of pHLIP was 2 μM and membrane-bound spectra correspond to lipid/peptide ratio of 200 (mol/mol). The excitation wavelength was 295 nm. Experiments were carried out at room temperature (~23 °C). See Section 2 for other details.

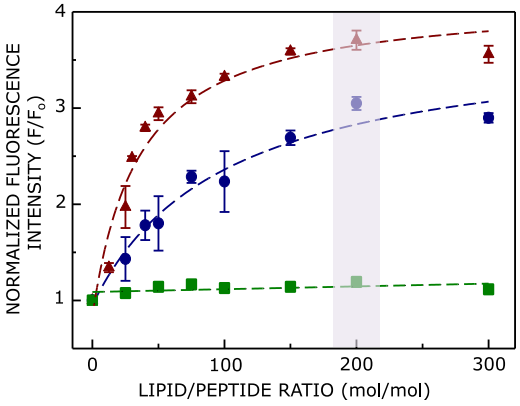

Fig. 3. Binding of pHLIP with ester and ether lipid membranes utilizing tryptophan fluorescence. Change in normalized fluorescence intensity with increasing lipid/peptide ratio (mol/mol) for DOPC (●) and DODPC (▲) membranes at pH 4. The lower plot (■) shows the change in normalized fluorescence intensity with increasing lipid/peptide ratio at pH 8 in case of DOPC membranes (data for DODPC membranes are similar and not shown). As evident from the binding plots, the normalized fluorescence intensity appears by and large constant, beyond lipid/peptide ratio of 200 (mol/mol, highlighted by a shaded box), thereby indicating that pHLIP is predominantly membrane-bound under these conditions. The concentration of pHLIP was 2 μM in all cases. The excitation wavelength was 295 nm. Experiments were carried out at room temperature (~23 °C). The dashed lines are obtained upon fitting the data points to Eq. (1) and the apparent dissociation constants for binding of pHLIP to ester and ether lipid membranes are shown in Table 1. See Section 2 for other details.

concentration, in both DOPC and DODPC membranes. As evident from the binding plots, the increase in normalized fluorescence intensity appears to stabilize beyond lipid/peptide ratio of 200 (mol/mol), thereby indicating that pHLIP is predominantly membrane-bound under these conditions. We therefore chose to carry out all fluorescence measurements under these conditions in which pHLIP was mostly bound to membranes.

The binding plots were analyzed and fitted to the classical Langmuir model for adsorption of ligand to multiple, equivalent, and non-interacting binding sites (Chakraborty et al., 2017) which provided apparent dissociation constant (K_d) for pHLIP binding to DOPC and DODPC membranes (shown in Table 1). Table 1 shows that K_d for pHLIP binding to DOPC membranes was ~3 times higher relative to K_d for

Table 1
Binding of pHLIP to ester and ether lipid membranes*.

Membrane type	Apparent dissociation constant (K_d)# (μM)
DOPC membranes	100.3 ± 18.8
DODPC membranes	33.2 ± 5.3

* Data shown are means ± SE of at least three independent measurements. See Section 2 for other details.
\# Calculated using Eq. (1).

pHLIP binding to DODPC membranes. This implies higher binding affinity of pHLIP in ether lipid (DODPC) membranes relative to that in ester lipid (DOPC) membranes. As a control, we repeated these measurements at pH 8, where pHLIP does not insert into the membrane. Fig. 3 shows that the fluorescence intensity of pHLIP remained invariant with increasing lipid/peptide ratio in ester lipid (DOPC) membranes at pH 8, thereby implying negligible change in pHLIP tryptophan microenvironment in the membrane-adsorbed (state II) form (similar data with ether lipids not shown). These results bring out the preferential interaction of pHLIP with ether lipids (see Discussion).

3.2. Restricted microenvironment of tryptophan residues in the membrane-inserted form of pHLIP in ester and ether lipid membranes

The hydration of ester and ether lipid membrane interface has been reported to be very different (Gawrisch et al., 1992; Guler et al., 2009). Since hydration at the lipid-protein interface plays a major role in lipid-protein interaction (Ho and Stubbs, 1992), we carried out red edge excitation shift (REES) measurements to monitor the microenvironment around tryptophans in membrane-inserted pHLIP in ester and ether lipid membranes. REES is conventionally defined as the shift in the wavelength of maximum fluorescence emission toward higher wavelengths, induced by a shift in the excitation wavelength toward the red edge of the absorption spectrum. REES gains relevance in motionally constrained environments where relaxation time of excited state dipoles in the solvent shell surrounding the fluorophore is equivalent to or longer than the fluorescence lifetime (Mukherjee and Chattopadhyay, 1995; Hof, 1999; Demchenko, 2002; Chattopadhyay, 2003; Raghuraman et al., 2005; Demchenko, 2008; Haldar et al., 2011; Chattopadhyay and Haldar, 2014). REES stems from relatively slow rates of solvent (water in biological systems) reorientation (compared to fluorescence lifetime) around an excited state fluorophore dipole, thereby allowing the monitoring of microenvironment-induced motional restriction imposed on water molecules in the immediate vicinity of the fluorophore. Hydration dynamics is important in the context of conformation of membrane peptides and proteins (Haldar and Chattopadhyay, 2012).

The shift in the maximum of fluorescence emission of membrane-inserted pHLIP as a function of excitation wavelength in ester and ether lipid membranes is shown in Fig. 4. Upon excitation at 280 nm, the tryptophans in membrane-inserted pHLIP at pH 4 display an emission maximum at 330 nm in both DOPC and DODPC membranes. The emission maximum exhibited a shift toward longer wavelengths when the excitation wavelength was progressively increased. In case of DOPC membranes, the emission maximum shifted to 338 nm when excited at 307 nm, resulting in a REES of 8 nm. The shift in the emission maximum was larger in case of pHLIP in DODPC membranes, since the emission maximum was 343 nm upon excitation at 307 nm. This corresponds to a REES of 13 nm. These values of REES are shown in the inset of Fig. 4. The differential magnitude of REES displayed by pHLIP in DOPC and DODPC membranes could be indicative of the difference in microenvironment of pHLIP tryptophans in these membranes.

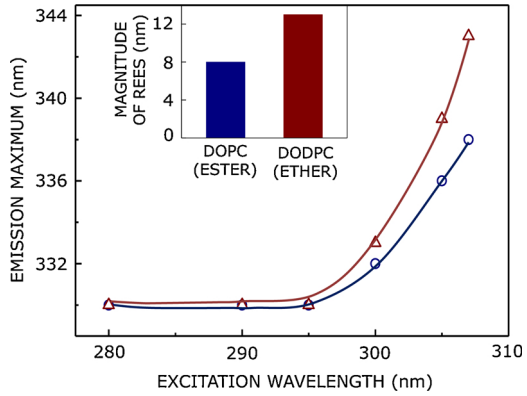

Fig. 4. Differential REES of pHLIP in ester and ether lipid membranes. Effect of changing excitation wavelength on the wavelength of maximum emission of pHLIP in DOPC (○) and DODPC (Δ) lipid membranes at pH 4. The inset shows the magnitude of REES of pHLIP tryptophans in DOPC and DODPC membranes. The magnitude of REES corresponds to the total shift in the emission maximum when the excitation wavelength is changed from 280 to 307 nm. The concentration of pHLIP was 2 μM and the lipid/peptide ratio was maintained at 200 (mol/mol, highlighted by the shaded box in Fig. 3, see legend to Fig. 3) to ensure that data correspond to a predominantly membrane-bound population of pHLIP. Experiments were carried out at room temperature (~23 °C). Lines joining the data points are provided merely as viewing guides. See Section 2 for other details.

3.3. Membrane penetration depths of pHLIP tryptophans in ester and ether lipid membranes

Tryptophan residues in membrane proteins and peptides typically exhibit interfacial localization in the membrane (Chattopadhyay et al., 1997; Killian and von Heijne, 2000; Kelkar and Chattopadhyay, 2006; Koeppe, 2007). The membrane interface is characterized by highest polarity and lowest mobility since there is a gradient of polarity and mobility along the bilayer normal (*i.e.*, the z-axis) (Chattopadhyay and Mukherjee, 1999; Haldar et al., 2011; Haldar and Chattopadhyay, 2012; Pal and Chattopadhyay, 2017). In order to examine the depth of tryptophan residues in membrane-inserted pHLIP in DOPC and DODPC membranes, we used the parallax method (Chattopadhyay and London, 1987) to determine the average penetration depth of pHLIP tryptophans in DOPC and DODPC membranes. The average depth of pHLIP tryptophans was calculated using the equation:

$$z_{cF} = L_{c1} + \{[(-1/\pi C) \ln (F_1/F_2) - L_{21}^2]/ 2 L_{21}\} \quad (2)$$

where z_{cF} is the average distance of the tryptophans from the center of the bilayer, L_{c1} is the distance of the shallow quencher from the center of the bilayer, L_{21} is difference in depth between the two quenchers and C is the two-dimensional quencher concentration (molecules/Å^2) in the plane of the membrane. Here, F_1/F_2 is the ratio of F_1/F_o and F_2/F_o, where F_1 and F_2 represent fluorescence intensities in presence of the shallow and deep quencher, respectively, both at the same quencher concentration C, and F_o is the fluorescence intensity without any quencher. All bilayer parameters used were the same as described previously (Chattopadhyay and London, 1987).

The average depths of penetration of tryptophan residues in the membrane-inserted form of pHLIP are shown in Table 2. The table shows that tryptophan residues of pHLIP are localized at the membrane interface, as apparent from average penetration depths of ~16 and ~15 Å from the center of the bilayer, in DOPC and DODPC membranes, respectively. The interfacial localization of tryptophans could facilitate appropriate interaction of pHLIP with DOPC and DODPC membranes (Kelkar and Chattopadhyay, 2006).

Table 2
Average membrane penetration depths of tryptophans of pHLIP in ester and ether lipid membranes[†].

Membrane type	Calculated distance from the bilayer center z_{cF} (Å)
DOPC membranes	~16
DODPC membranes	~15

[†] Depths were calculated from fluorescence quenchings obtained with samples containing 10 mol% of Tempo- and 5-PC and using Eq. (2). Samples were excited at 295 nm and emission was collected at 330 nm. The lipid/peptide ratio was 200 (mol/mol) and the concentration of pHLIP was 1.6 μM in all cases. See Section 2 for other details.

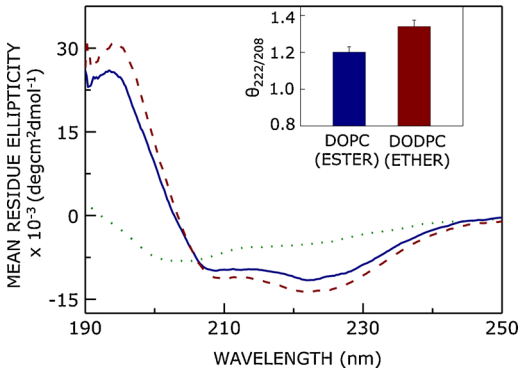

Fig. 5. Secondary structure of pHLIP in ester and ether lipid membranes. Representative far-UV CD spectra of pHLIP in DOPC (—), DODPC (- - -) membranes and in buffer (·····) at pH 4. The inset shows the increase in helicity (calculated as ratio of mean residue ellipticities at 222 and 208 nm) of pHLIP in DODPC membranes, relative to DOPC membranes. The concentration of peptide was 5 μM in all cases, and the lipid/peptide ratio was 150 (mol/mol). Experiments were carried out at room temperature (~23 °C). See Section 2 for other details.

3.4. Secondary structure of membrane-inserted pHLIP in ester and ether lipid membranes

As stated above, pHLIP is known to adopt α-helical conformation in membranes upon lowering the pH to 4 (Reshetnyak et al., 2007). Fig. 5 shows that pHLIP adopts an α-helical structure (characterized by peaks at 208 and 222 nm) in both DOPC and DODPC membranes. Interestingly, Fig. 5 shows an increase in the helicity of pHLIP (~10 %) in DODPC membranes relative to DOPC membranes, as estimated by the ratio of mean residue ellipticities at 222 and 208 nm (see inset). Further analysis using the DichroWeb tool revealed ~8 % higher α-helical content of pHLIP in DODPC membranes relative to DOPC membranes (see Table S1). The increased helicity of pHLIP in ether lipid membranes could be correlated with increased REES in these membranes (Fig. 4). These observations assume relevance in the context of previous reports showing that the restricted microenvironment experienced by tryptophan residues localized at the membrane interface could act as a sensitive indicator of peptide secondary structure (Chattopadhyay et al., 2003; Chattopadhyay and Haldar, 2014; Chakraborty and Chattopadhyay, 2017; Pal et al., 2018).

4. Discussion

The interaction of peptides with membranes is implicated in several important membrane-associated biological phenomena that include the action of antimicrobial peptides, hormone-receptor interactions and viral fusion (Raghuraman and Chattopadhyay, 2007; Kelkar and Chattopadhyay, 2007; Galdiero et al., 2013; Herrera et al., 2016). In this work, we explored the differential interaction of pHLIP with representative ester (DOPC) and ether (DODPC) lipid membranes

utilizing fluorescence and CD spectroscopic approaches. The choice of lipids ensured that only the interfacial chemistry of the membrane is altered from ester- to ether-type linkage (Fig. 1b,c), without changing the lipid headgroup or acyl chain length. The pH-dependent insertion of pHLIP into membranes is an interesting aspect of the peptide which provides the opportunity for imaging tumor tissue and targeted drug delivery (Reshetnyak et al., 2011; Adochite et al., 2014; Deacon et al., 2015; Burns et al., 2015; Wyatt et al., 2017; Rinaldi et al., 2018; Son et al., 2019). In this context, exploring the mechanism of pHLIP-membrane interaction assumes relevance since it could help in optimizing therapeutic strategies for the effective application of pHLIP. While there is extensive literature on the application of pHLIP for imaging tumor tissue and targeted drug delivery, relatively less is known about the molecular mechanism and biophysical basis of pHLIP-membrane interaction (Barrera et al., 2012; Kyrychenko et al., 2015; Scott et al., 2015; Karabadzhak et al., 2018; Westerfield et al., 2019; Scott et al., 2019). Our results on the interaction of pHLIP with ester and ether lipid membranes is relevant in this backdrop.

Our results show that pHLIP exhibits higher affinity (~3 times) to ether lipid membranes relative to ester lipid membranes. In addition, pHLIP tryptophans exhibited differential extent of REES in membranes of ester and ether lipids, with increased REES observed for pHLIP in ether (DODPC) lipid membranes. This indicates that the local microenvironment around pHLIP tryptophans are different in these membranes and more restricted (in terms of restriction of interfacial water molecules) in case of ether lipid membranes. This was accompanied by an increase in the helicity of pHLIP when bound to ether lipid membranes relative to ester lipid membranes. In a parenthetical fashion, we note that the difference in REES and CD data for pHLIP in ester and ether lipid membranes could represent an upper limit, due to slightly different amounts of bound peptide in these membranes. Taken together, these results show preference of pHLIP for ether lipids. A schematic representation of differential interaction of pHLIP in ester *vs* ether lipid membranes is shown in Fig. 6. Our results assume significance in view of the fact that purple membrane of *Halobacterium halobium* (which serves as the native membrane for bacteriorhodopsin, from which pHLIP is derived) is enriched with ether lipids (Kates et al., 1965; Marshall and Brown, 1968; Henderson, 1977; Renner et al., 2005).

The differential interaction and binding of pHLIP with ester and ether lipid membranes could have its origin in the intrinsic differences in physicochemical properties of the membrane interface, depending on the type of linkage (*e.g.*, ester or ether) of the constituent lipids. A fundamental difference between ester and ether lipids is the different hybridization state (and therefore geometry) of the sp^2 carbon of the carbonyl group in ester lipids and the sp^3 carbon of the ether linkage (Mukherjee and Chattopadhyay, 2005). This change in lipid molecular structure results in increased hydration in ether phospholipids. The physicochemical aspects of interfacial water molecules in ester and ether lipid membranes have been previously monitored utilizing fluorescence and other spectroscopic approaches (Sommer et al., 1990; Gawrisch et al., 1992; Hutterer et al., 1997; Mukherjee and Chattopadhyay, 2005; Guler et al., 2009; Balleza et al., 2014; Aloi et al., 2017). Slightly increased water penetration (Smaby et al., 1983; Sommer et al., 1990; Lewis et al., 1996) and the ordered nature of water molecules (Guler et al., 2009) in ether lipid membranes relative to ester lipid membranes have been reported. Previous work by us and others, utilizing fluorescence spectroscopy, has shown differences in emission maximum, fluorescence lifetimes and anisotropy of interfacial probes in ether lipid membranes relative to ester lipid membranes. These results indicate tighter packing and a more polar environment in ether lipid membranes (Sommer et al., 1990; Hutterer et al., 1997; Mukherjee and Chattopadhyay, 2005; Balleza et al., 2014). In addition, these results are supported by molecular dynamics simulations which show that water in the interfacial region of ether membranes is more restricted, exhibiting slower translational and rotational motion relative to ester

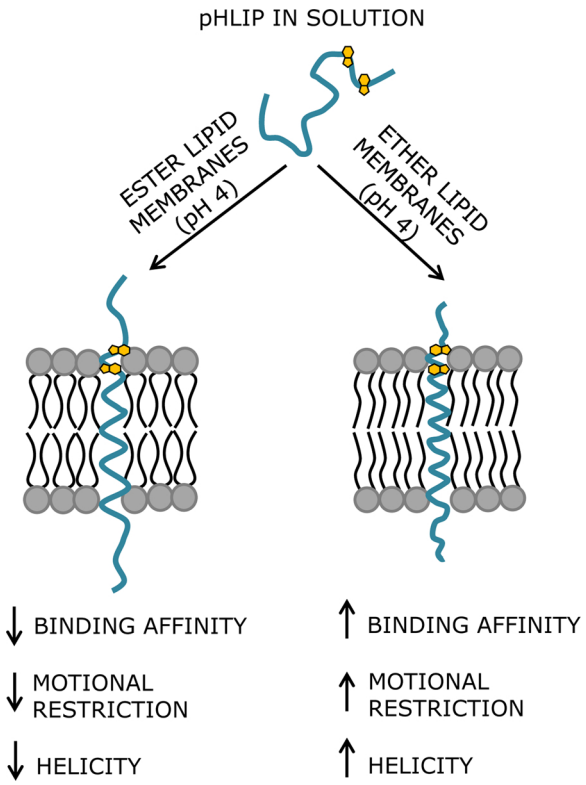

Fig. 6. Differential interaction of pHLIP with ester and ether lipid membranes. A schematic representation of the differential sensitivity of pHLIP in representative ester and ether lipid membranes at pH 4. In ether lipid membranes, pHLIP exhibited a higher binding affinity, enhanced motional restriction in the microenvironment and increase in peptide helicity. The tryptophans at positions 9 and 15 are highlighted.

lipid membranes (Shinoda et al., 2004; Kruczek et al., 2017). In addition, membrane dipole potential has been reported to be different in ester and ether lipid membranes (Gawrisch et al., 1992; Shinoda et al., 2004; Lairion and Disalvo, 2007; Berkovich et al., 2012; Kruczek et al., 2017; Shen et al., 2019). Membrane dipole potential is the electrostatic potential difference within the membrane bilayer due to the non-random arrangement of amphiphile dipoles and water molecules at the membrane interface (Clarke, 2001; Sarkar et al., 2017). Taken together, the modulation in the interaction of pHLIP with DOPC and DODPC membranes, in terms of binding affinity, restricted microenvironment and peptide conformation, could be attributed to higher membrane order, increased water penetration and possibly lower dipole potential in ether lipid membranes.

These results assume relevance in view of the fact that ether lipids are known to be elevated in cancer tissues and have emerged as potential biomarkers of various pathophysiological conditions, including cancer, neurodegenerative diseases and metabolic disorders (Snyder and Wood, 1969; Howard et al., 1972; Albert and Anderson, 1977; Roos and Choppin, 1984; Benjamin et al., 2013; Jaffrès et al., 2016; Dean and Lodhi, 2018; Vidavsky et al., 2019). We envision that insight into the lipid binding specificity of pHLIP, *e.g.*, higher affinity of pHLIP toward ether-linked membranes, could be utilized to better engineer pHLIP to improve translocation across membranes for more efficient therapeutic use in disease conditions.

Declaration of Competing Interest

The authors declare that there is no conflict of interest.

Acknowledgments

This work was supported by the Council of Scientific and Industrial Research (Govt. of India). A.C. gratefully acknowledges support from SERB Distinguished Fellowship (Department of Science and Technology, Govt. of India). We sincerely thank Dr. Sandro Keller (Technische Universität Kaiserslautern, Germany) for the kind gift of pHLIP. B.D.R. thanks the University Grants Commission for the award of a Senior Research Fellowship. H.C. and Ar.C. thank the Council of Scientific and Industrial Research for the award of Senior Research Associateship and Senior Research Fellowship, respectively. A.C. is a Distinguished Visiting Professor at Indian Institute of Technology Bombay (Mumbai), and Adjunct Professor at RMIT University (Melbourne, Australia), Tata Institute of Fundamental Research (Mumbai) and Indian Institute of Science Education and Research (Kolkata), and an Honorary Professor at the Jawaharlal Nehru Centre for Advanced Scientific Research (Bangalore). We thank Sreetama Pal for useful discussion, and members of the Chattopadhyay laboratory for critically reading the manuscript.

Appendix A. Supplementary data

Supplementary material related to this article can be found, in the online version, at doi:https://doi.org/10.1016/j.chemphyslip.2019.104849.

References

Abrams, F.S., London, E., 1993. Extension of the parallax analysis of membrane penetration depth to the polar region of model membranes: use of fluorescence quenching by a spin-label attached to the phospholipid polar headgroup. Biochemistry 32, 10826–10831.
Adochite, R.-C., Moshnikova, A., Carlin, S.D., Guerrieri, R.A., Andreev, O.A., Lewis, J.S., Reshetnyak, Y.K., 2014. Targeting breast tumors with pH (Low) insertion peptides. Mol. Pharm. 11, 2896–2905.
Albert, D.H., Anderson, C.E., 1977. Ether-linked glycerolipids in human brain tumors. Lipids 12, 188–192.
Aloi, E., Oranges, M., Guzzi, R., Bartucci, R., 2017. Low-temperature dynamics of chain-labeled lipids in ester- and ether-linked phosphatidylcholine membranes. J. Phys. Chem. B 121, 9239–9246.
An, M., Wijesinghe, D., Andreev, O.A., Reshetnyak, Y.K., Engelman, D.M., 2010. pH-(low)-insertion-peptide (pHLIP) translocation of membrane impermeable phalloidin toxin inhibits cancer cell proliferation. Proc. Natl. Acad. Sci. U.S.A. 107, 20246–20250.
Andreev, O.A., Dupuy, A.D., Segala, M., Sandugu, S., Serra, D.A., Chichester, C.O., Engelman, D.M., Reshetnyak, Y.K., 2007. Mechanism and uses of a membrane peptide that targets tumors and other acidic tissues in vivo. Proc. Natl. Acad. Sci. U.S.A. 104, 7893–7898.
Andreev, O.A., Karabadzhak, A.G., Weerakkody, D., Andreev, G.O., Engelman, D.M., Reshetnyak, Y.K., 2010. pH (low) insertion peptide (pHLIP) inserts across a lipid bilayer as a helix and exits by a different path. Proc. Natl. Acad. Sci. U.S.A. 107, 4081–4086.
Balleza, D., Garcia-Arribas, A.B., Sot, J., Ruiz-Mirazo, K., Goñi, F.M., 2014. Ether- versus ester-linked phospholipid bilayers containing either linear or branched apolar chains. Biophys. J. 107, 1364–1374.
Barrera, F.N., Fendos, J., Engelman, D.M., 2012. Membrane physical properties influence transmembrane helix formation. Proc. Natl. Acad. Sci. U.S.A. 109, 14422–14427.
Benjamin, D.I., Cozzo, A., Ji, X., Roberts, L.S., Louie, S.M., Mulvihill, M.M., Luo, K., Nomura, D.K., 2013. Ether lipid generating enzyme AGPS alters the balance of structural and signaling lipids to fuel cancer pathogenicity. Proc. Natl. Acad. Sci. U.S.A. 110, 14912–14917.
Berkovich, A.K., Lukashev, E.P., Melik-Nubarov, N.S., 2012. Dipole potential as a driving force for the membrane insertion of polyacrylic acid in slightly acidic milieu. Biochim. Biophys. Acta 1818, 375–383.
Burns, K.E., Robinson, M.K., Thévenin, D., 2015. Inhibition of cancer cell proliferation and breast tumor targeting of pHLIP-monomethyl auristatin E conjugates. Mol. Pharm. 12, 1250–1258.
Chakraborty, H., Chattopadhyay, A., 2017. Sensing tryptophan microenvironment of amyloid protein utilizing wavelength-selective fluorescence approach. J. Fluoresc. 27, 1995–2000.
Chakraborty, H., Lentz, B.R., Kombrabail, M., Krishnamoorthy, G., Chattopadhyay, A., 2017. Depth-dependent membrane ordering by hemagglutinin fusion peptide promotes fusion. J. Phys. Chem. B 121, 1640–1648.
Chattopadhyay, A., 2003. Exploring membrane organization and dynamics by the wavelength-selective fluorescence approach. Chem. Phys. Lipids 122, 3–17.
Chattopadhyay, A., Arora, A., Kelkar, D.A., 2005. Dynamics of a membrane-bound tryptophan analog in environments of varying hydration: a fluorescence approach. Eur. Biophys. J. 35, 62–71.
Chattopadhyay, A., Haldar, S., 2014. Dynamic insight into protein structure utilizing red edge excitation shift. Acc. Chem. Res. 47, 12–19.
Chattopadhyay, A., London, E., 1987. Parallax method for direct measurement of membrane penetration depth utilizing fluorescence quenching by spin-labeled phospholipids. Biochemistry 26, 39–45.
Chattopadhyay, A., Mukherjee, S., 1999. Depth-dependent solvent relaxation in membranes: wavelength-selective fluorescence as a membrane dipstick. Langmuir 15, 2142–2148.
Chattopadhyay, A., Mukherjee, S., Rukmini, R., Rawat, S.S., Sudha, S., 1997. Ionization, partitioning and dynamics of tryptophan octyl ester: implications for membrane-bound tryptophan residues. Biophys. J. 73, 839–849.
Chattopadhyay, A., Raghuraman, H., 2004. Application of fluorescence spectroscopy to membrane protein structure and dynamics. Curr. Sci. 87, 175–180.
Chattopadhyay, A., Rawat, S.S., Kelkar, D.A., Ray, S., Chakrabarti, A., 2003. Organization and dynamics of tryptophan residues in erythroid spectrin: novel structural features of denatured spectrin revealed by the wavelength-selective fluorescence approach. Protein Sci. 12, 2389–2403.
Chaudhuri, A., Chattopadhyay, A., 2014. Lipid binding specificity of bovine α-lactalbumin: a multidimensional approach. Biochim. Biophys. Acta 1838, 2078–2086.
Chen, G.C., Yang, J.T., 1977. Two-point calibration of circular dichrometer with d-10-camphorsulfonic acid. Anal. Lett. 10, 1195–1207.
Clarke, R.J., 2001. The dipole potential of phospholipid membranes and methods for its detection. Adv. Colloid Interface Sci. 89-90, 263–281.
Dailey, M.M., Hait, C., Holt, P.A., Maguire, J.M., Meier, J.B., Miller, M.C., Petraccone, L., Trent, J.O., 2009. Structure-based drug design: from nucleic acid to membrane protein targets. Exp. Mol. Pathol. 86, 141–150.
Deacon, J.C., Engelman, D.M., Barrera, F.N., 2015. Targeting acidity in diseased tissues: mechanism and applications of the membrane-inserting peptide, pHLIP. Arch. Biochem. Biophys. 565, 40–48.
Dean, J.M., Lodhi, I.J., 2018. Structural and functional roles of ether lipids. Protein Cell 9, 196–206.
Demchenko, A.P., 2002. The red-edge effects: 30 years of exploration. Luminescence 17, 19–42.
Demchenko, A.P., 2008. Site-selective red-edge effects. Methods Enzymol. 450, 59–78.
Drews, J., 2000. Drug discovery: a historical perspective. Science 287, 1960–1964.
Eftink, M.R., 1991. Fluorescence techniques for studying protein structure. Methods Biochem. Anal. 35, 127–205.
Fendos, J., Barrera, F.N., Engelman, D.M., 2013. Aspartate embedding depth affects pHLIP's insertion pKa. Biochemistry 52, 4595–4604.
Galdiero, S., Falanga, A., Cantisani, M., Vitiello, M., Morelli, G., Galdiero, M., 2013. Peptide-lipid interactions: experiments and applications. Int. J. Mol. Sci. 14, 18758–18789.
Gawrisch, K., Ruston, D., Zimmerberg, J., Parsegian, V.A., Rand, R.P., Fuller, N., 1992. Membrane dipole potentials, hydration forces, and the ordering of water at membrane surfaces. Biophys. J. 61, 1213–1223.
Guler, S.D., Ghosh, D.D., Pan, J., Mathai, J.C., Zeidel, M.L., Nagle, J.F., Tristram-Nagle, S., 2009. Effects of ether vs. ester linkage on lipid bilayer structure and water permeability. Chem. Phys. Lipids 160, 33–44.
Haldar, S., Chattopadhyay, A., 2012. Hydration dynamics of probes and peptides in captivity. In: Geddes, C.D. (Ed.), Reviews in Fluorescence 2010. Springer, New York, pp. 155–172.
Haldar, S., Chaudhuri, A., Chattopadhyay, A., 2011. Organization and dynamics of membrane probes and proteins utilizing the red edge excitation shift. J. Phys. Chem. B 115, 5693–5706.
Henderson, R., 1977. The purple membrane from Halobacterium halobium. Ann. Rev. Biophys. Bioeng. 6, 87–109.
Herrera, A., Tomich, J.M., Prakash, O., 2016. Membrane-interacting peptides: a review. Curr. Protein Pept. Sci. 17, 827–841.
Ho, C., Stubbs, C.D., 1992. Hydration at the membrane protein-lipid interface. Biophys. J. 63, 897–902.
Hof, M., 1999. Solvent relaxation in biomembranes. In: Retting, W., Strehmel, B., Schrader, S., Seifert, H. (Eds.), Applied Fluorescence in Chemistry, Biology and Medicine. Springer, New York, pp. 439–456.
Howard, B.V., Morris, H.P., Bailey, J.M., 1972. Ether-lipids, α-glycerol phosphate dehydrogenase, and growth rate in tumors and cultured cells. Cancer Res. 32, 1533–1538.
Hunt, J.F., Rath, P., Rothschild, K.J., Engelman, D.M., 1997. Spontaneous, pH-dependent membrane insertion of a transbilayer α-helix. Biochemistry 36, 15177–15192.
Hutterer, R., Schneider, F.W., Hof, M., 1997. Time-resolved emission spectra and anisotropy profiles for symmetric diacyl- and dietherphosphatidylcholines. J. Flouresc. 7, 27–33.
Jaffrès, P.-A., Gajate, C., Bouchet, A.M., Couthon-Gourvès, H., Chantôme, A., Potier-Cartereau, M., Besson, P., Bougnoux, P., Mollinedo, F., Vandier, C., 2016. Alkyl ether lipids, ion channels and lipid raft reorganization in cancer therapy. Pharmacol. Ther. 165, 114–131.
Jafurulla, M., Kumar, G.A., Rao, B.D., Chattopadhyay, A., 2019. A critical analysis of molecular mechanisms underlying membrane cholesterol sensitivity of GPCRs. Adv. Exp. Med. Biol. 1115, 21–52.
Karabadzhak, A.G., Weerakkody, D., Andreev, O.A., Reshetnyak, Y.K., Engelman, D.M., 2018. Bilayer thickness and curvature influence binding and insertion of a pHLIP peptide. Biophys. J. 114, 2107–2115.
Karabadzhak, A.G., Weerakkody, D., Wijesinghe, D., Thakur, M.S., Engelman, D.M., Andreev, O.A., Markin, V.S., Reshetnyak, Y.K., 2012. Modulation of the pHLIP transmembrane helix insertion pathway. Biophys. J. 102, 1846–1855.
Kates, M., Yengoyan, L.S., Sastry, P.S., 1965. A diether analog of phosphatidyl glycerophosphate in Halobacterium cutirubrum. Biochim. Biophys. Acta 98, 252–268.

Kelkar, D.A., Chattopadhyay, A., 2006. Membrane interfacial localization of aromatic amino acids and membrane protein function. J. Biosci. 31, 297–302.
Kelkar, D.A., Chattopadhyay, A., 2007. The gramicidin ion channel: a model membrane protein. Biochim. Biophys. Acta 1768, 2011–2025.
Killian, J.A., von Heijne, G., 2000. How proteins adapt to a membrane-water interface. Trends Biochem. Sci. 25, 429–434.
Kirby, E.P., Steiner, R.F., 1970. The influence of solvent and temperature upon the fluorescence of indole derivatives. J. Phys. Chem. 74, 4480–4490.
Koeppe II, R.E., 2007. Concerning tryptophan and protein-bilayer interactions. J. Gen. Physiol. 130, 223–224.
Kremer, J.M.H., van der Esker, M.W., Pathmamanoharan, C., Wiersema, P.H., 1977. Vesicles of variable diameter prepared by a modified injection method. Biochemistry 16, 3932–3935.
Kruczek, J., Saunders, M., Khosla, M., Tu, Y., Pandit, S.A., 2017. Molecular dynamics simulations of ether- and ester-linked phospholipids. Biochim. Biophys. Acta 1859, 2297–2307.
Kyrychenko, A., Vasquez-Montes, V., Ulmschneider, M.B., Ladokhin, A.S., 2015. Lipid headgroups modulate membrane insertion of pHLIP peptide. Biophys. J. 108, 791–794.
Lairion, F., Disalvo, E.A., 2007. Effect of arbutin on the dipole potential and area per lipid of ester and ether phosphatidylcholine and phosphatidyl ethanolamine monolayers. Biochim. Biophys. Acta 1768, 450–456.
Lee, A.G., 2004. How lipids affect the activities of integral membrane proteins. Biochim. Biophys. Acta 1666, 62–87.
Lees, J.G., Miles, A.J., Wien, F., Wallace, B.A., 2006. A reference database for circular dichroism spectroscopy covering fold and secondary structure space. Bioinformatics 22, 1955–1962.
Lewis, R.N.A.H., Pohle, W., McElhaney, R.N., 1996. The interfacial structure of phospholipid bilayers: differential scanning calorimetry and fourier transform infrared spectroscopic studies of 1,2-dipalmitoyl-sn-glycero-3-phosphorylcholine and its dialkyl and acyl-alkyl analogs. Biophys. J. 70, 2736–2746.
Marshall, C.L., Brown, A.D., 1968. The membrane lipids of Halobacterium halobium. Biochem. J. 110, 441–448.
Mattjus, P., Bittman, R., Slotte, J.P., 1996. Molecular interaction and lateral domain formation in monolayers containing cholesterol and phosphatidylcholines with acyl- or alkyl-linked C16 chains. Langmuir 12, 1284–1290.
Mukherjee, S., Chattopadhyay, A., 1995. Wavelength-selective fluorescence as a novel tool to study organization and dynamics in complex biological systems. J. Fluoresc. 5, 237–246.
Mukherjee, S., Chattopadhyay, A., 2005. Influence of ester and ether linkage in phospholipids on the environment and dynamics of the membrane interface: a wavelength-selective fluorescence approach. Langmuir 21, 287–293.
Otieno, S.A., Hanz, S.Z., Chakravorty, B., Zhang, A., Klees, L.M., An, M., Qiang, W., 2018. pH-dependent thermodynamic intermediates of pHLIP membrane insertion determined by solid-state NMR spectroscopy. Proc. Natl. Acad. Sci. U.S.A. 115, 12194–12199.
Pal, S., Aute, R., Sarkar, P., Bose, S., Deshmukh, M.V., Chattopadhyay, A., 2018. Constrained dynamics of the sole tryptophan in the third intracellular loop of the serotonin$_{1A}$ receptor. Biophys. Chem. 240, 34–41.
Pal, S., Chattopadhyay, A., 2017. What is so unique about biomembrane organization and dynamics? In: Chattoapdhyay, A. (Ed.), Membrane Organization and Dynamics. Springer Series in Biophysics. Springer International Publishing, pp. 1–9.
Raghuraman, H., Chattopadhyay, A., 2007. Melittin: a membrane-active peptide with diverse functions. Biosci. Rep. 27, 189–223.
Raghuraman, H., Kelkar, D.A., Chattopadhyay, A., 2005. Novel insights into protein structure and dynamics utilizing the red edge excitation shift approach. In: Geddes, C.D., Lakowicz, J.R. (Eds.), Reviews in Fluorescence 2005. Springer, New York, pp. 199–222.
Rao, B.D., Chakraborty, H., Keller, S., Chattopadhyay, A., 2018. Aggregation behavior of pHLIP in aqueous solution at low concentrations: a fluorescence study. J. Fluoresc. 28, 967–973.
Renner, C., Kessler, B., Oesterhelt, D., 2005. Lipid composition of integral purple membrane by ^{1}H and ^{31}P NMR. J. Lipid Res. 46, 1755–1764.
Reshetnyak, Y.K., Andreev, O.A., Lehnert, U., Engelman, D.M., 2006. Translocation of molecules into cells by pH-dependent insertion of a transmembrane helix. Proc. Natl. Acad. Sci. U.S.A. 103, 6460–6465.
Reshetnyak, Y.K., Andreev, O.A., Segala, M., Markin, V.S., Engelman, D.M., 2008. Energetics of peptide (pHLIP) binding to and folding across a lipid bilayer membrane. Proc. Natl. Acad. Sci. U.S.A. 105, 15340–15345.
Reshetnyak, Y.K., Segala, M., Andreev, O.A., Engelman, D.M., 2007. A monomeric membrane peptide that lives in three worlds: in solution, attached to, and inserted across lipid bilayers. Biophys. J. 93, 2363–2372.
Reshetnyak, Y.K., Yao, L., Zheng, S., Kuznetsov, S., Engelman, D.M., Andreev, O.A., 2011. Measuring tumor aggressiveness and targeting metastatic lesions with fluorescent pHLIP. Mol. Imaging Biol. 13, 1146–1156.
Rinaldi, F., Hanieh, P.N., Del Favero, E., Rondelli, V., Brocca, P., Pereira, M.C., Andreev, O.A., Reshetnyak, Y.K., Marianecci, C., Carafa, M., 2018. Decoration of nanovesicles with pH (low) insertion peptide (pHLIP) for targeted delivery. Nanoscale Res. Lett. 13, 391.
Roos, D.S., Choppin, P.W., 1984. Tumorigenicity of cell lines with altered lipid composition. Proc. Natl. Acad. Sci. U.S.A. 81, 7622–7626.
Sanderson, J.M., 2005. Peptide-lipid interactions: insights and perspectives. Org. Biomol. Chem. 3, 201–212.
Sarkar, P., Chakraborty, H., Chattopadhyay, A., 2017. Differential membrane dipolar orientation induced by acute and chronic cholesterol depletion. Sci. Rep. 7, 4484.
Scott, H.L., Heberle, F.A., Katsaras, J., Barrera, F.N., 2019. Phosphatidylserine asymmetry promotes the membrane insertion of a transmembrane helix. Biophys. J. 116, 1495–1506.
Scott, H.L., Nguyen, V.P., Alves, D.S., Davis, F.L., Booth, K.R., Bryner, J., Barrera, F.N., 2015. The negative charge of the membrane has opposite effects on the membrane entry and exit of pH-low insertion peptide. Biochemistry 54, 1709–1712.
Scott, H.L., Westerfield, J.M., Barrera, F.N., 2017. Determination of the membrane translocation pK of the pH-low insertion peptide. Biophys. J. 113, 869–879.
Shen, H., Zhao, K., Wu, Z., 2019. Effects of ether-linkage on membrane dipole potential and cholesterol flip-flop motion in lipid bilayer membranes. J. Phys. Chem. B 123, 7818–7828.
Shinoda, K., Shinoda, W., Baba, T., Mikami, M., 2004. Comparative molecular dynamics study of ether- and ester-linked phospholipid bilayers. J. Chem. Phys. 121, 9648–9654.
Smaby, J.M., Hermetter, A., Schmid, P.C., Paltauf, F., Brockman, H.L., 1983. Packing of ether and ester phospholipids in monolayers. Evidence for hydrogen-bonded water at the sn-1 acyl group of phosphatidylcholines. Biochemistry 22, 5808–5813.
Snyder, F., Wood, R., 1969. Alkyl and alk-1-enyl ethers of glycerol in lipids from normal and neoplastic human tissues. Cancer Res. 29, 251–257.
Sommer, A., Paltauf, F., Hermetter, A., 1990. Dipolar solvent relaxation on a nanosecond time scale in ether phospholipid membranes as determined by multifrequency phase and modulation fluorometry. Biochemistry 29, 11134–11140.
Son, S.-M., Yun, J., Lee, S.-H., Han, H.S., Lim, Y.H., Woo, C.G., Lee, H.-C., Song, H.G., Gu, Y.-M., Lee, H.-J., Lee, O.-J., 2019. Therapeutic effect of pHLIP-mediated CEACAM6 gene silencing in lung adenocarcinoma. Sci. Rep. 9, 11607.
Sreerama, N., Woody, R.W., 2000. Estimation of protein secondary structure from circular dichroism spectra: comparison of CONTIN, SELCON and CDSSTR methods with an expanded reference set. Anal. Biochem. 287, 252–260.
Tang, J., Gai, F., 2008. Dissecting the membrane binding and insertion kinetics of a pHLIP peptide. Biochemistry 47, 8250–8252.
Thévenin, D., An, M., Engelman, D.M., 2009. pHLIP-mediated translocation of membrane-impermeable molecules into cells. Chem. Biol. 16, 754–762.
Vidavsky, N., Kunitake, J.A.M.R., Diaz-Rubio, M.E., Chiou, A.E., Loh, H.-C., Zhang, S., Masic, A., Fischbach, C., Estroff, L.A., 2019. Mapping and profiling lipid distribution in a 3D model of breast cancer progression. ACS Cent. Sci. 5, 768–780.
Westerfield, J., Gupta, C., Scott, H.L., Ye, Y., Cameron, A., Mertz, B., Barrera, F.N., 2019. Ions modulate key interactions between pHLIP and lipid membranes. Biophys. J. 117, 920–929.
Whitmore, L., Wallace, B.A., 2004. DICHROWEB, an online server for protein secondary structure analyses from circular dichroism spectroscopic data. Nucleic Acids Res. 32, W668–W673.
Whitmore, L., Wallace, B.A., 2008. Protein secondary structure analyses from circular dichroism spectroscopy: methods and reference databases. Biopolymers 89, 392–400.
Wyatt, L.C., Lewis, J.S., Andreev, O.A., Reshetnyak, Y.K., Engelman, D.M., 2017. Applications of pHLIP technology for cancer imaging and therapy. Trends Biotechnol. 35, 653–664.
Zoonens, M., Reshetnyak, Y.K., Engelman, D.M., 2008. Bilayer interactions of pHLIP, a peptide that can deliver drugs and target tumors. Biophys. J. 95, 225–235.